Inorganic Chemistry

Article

pubs.acs.org/IC

Coordinated Aqua vs Methanol Substitution Kinetics in *fac*-Re(I) Tricarbonyl Tropolonato Complexes

Marietjie Schutte, Andreas Roodt, and Hendrik G. Visser*

Department of Chemistry, University of the Free State, P.O. Box 339, Bloemfontein, 9300, South Africa

Supporting Information

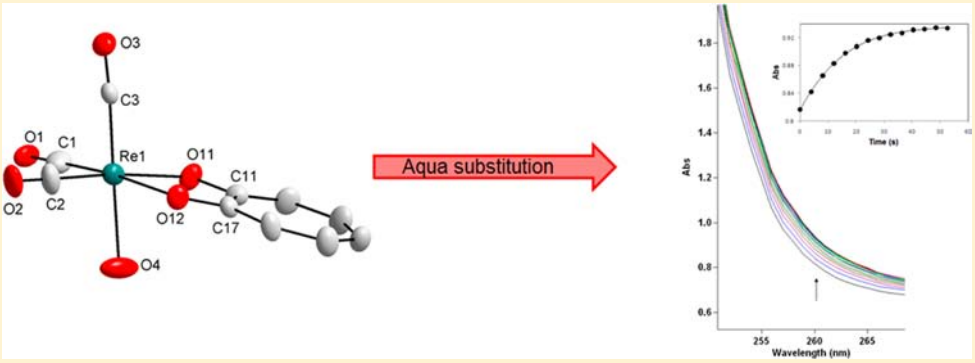

ABSTRACT: Water-soluble *fac*-[$Re(CO)_3$(L,L′-Bid)(X)] (L,L′-Bid = tropolonato, X = H_2O, methanol) complexes have been synthesized, and the aqua and methanol substitution reactions were investigated in water (pH range 6.3−10.0) and methanol, respectively, and compared. Thiocyanate ions were used as monodentate entering ligand. The complexes were characterized by UV−vis, IR, and NMR spectroscopy. The crystal structures of the complexes [NEt_4] *fac*-[Re(Trop)$(CO)_3(H_2O)$].NO_3.H_2O (reactant) and *fac*-[$Re(CO)_3$(Trop)(Py)], a substitution product, are reported. Overall it was found that the aqua substitution of *fac*-[$Re(CO)_3$(Trop)(H_2O)] is about 10 times faster than the methanol substitution reaction for *fac*-[$Re(CO)_3$(Trop)(MeOH)], with forward and reverse rate and stability constants [k_1 (M^{-1} s^{-1}), k_{-1} (s^{-1}), K_1, (M^{-1})] for thiocyanate as monodentate entering ligand as follows: *fac*-[$Re(CO)_3$(Trop)(H_2O)] = 2.54 ± 0.03, 0.0077 ± 0.0005, 330 ± 22/207 ± 14 and *fac*-[$Re(CO)_3$(Trop)(MeOH)] = 0.268 ± 0.002, 0.0044 ± 0.0002, (61 ± 3)/(52 ± 4). The activation parameters [$\Delta H^{\ddagger}_{k1}$ (kJ mol^{-1}), $\Delta S^{\ddagger}_{k1}$ (J K^{-1} mol^{-1})] for the aqua and methanol complex respectively are 56.1 ± 0.7, −49 ± 2 and 64 ± 1, −43 ± 5.

INTRODUCTION

There is currently significant interest in the *fac*-$[M(CO)_3]^+$ entity [M = Re(I), Tc(I)] for possible use in diagnostic and therapeutic radiopharmacy. The reasons for this are multifold and range from its compact size to its low positive charge, coordination properties, d^6 low-spin configuration, and significant stability.[1−6] The synthesis of *fac*-[^{99m}Tc-$(CO)_3(H_2O)_3$] in aqueous medium and under mild conditions by Alberto et al.[6] further increased the focus on this metal core, especially as it readily reacts with bidentate and tridentate ligand chelators to form stable complexes. It is a versatile synthon for the labeling of different bioactive molecules, recombinant proteins, and small molecules.[7] A one-step kit formulation is available for the synthesis of *fac*-[^{99m}Tc$(CO)_3]^+$, and a two-step kit is in development for the synthesis of *fac*-[^{188}Re$(CO)_3]^+$.[8−10]

A principal reason for the interest and the use of the *fac*-$[M(CO)_3(H_2O)_3]^+$ synthon in radiopharmacy is the stable *fac*-rhenium tricarbonyl core and the three labile sites occupied by water molecules. These sites can easily be replaced by different ligands and ligand combinations.[11−15] Despite all the favorable properties of *fac*-$[M(CO)_3]^+$ in the use of potential therapeutic and imaging agents, one of the biggest challenges is to develop a chelator that complexes strongly to the metal but has a minimal effect on the properties of the biomolecule. The chelator should have a high affinity for the metal core and form thermodynamic and kinetic stable complexes and must have complete complexation to *fac*-[^{99m}Tc$(CO)_3]^+$ at a ligand concentration of 10^{-5}−10^{-4} M. The latter prerequisite is important when labeling receptor ligands like steroids and small peptides, since the free receptor sites may be saturated with unlabeled biomolecules at ligand concentrations higher than 10^{-4} M and will therefore decrease the selectivity of the radionuclide accumulation in the target tissue.

The aqueous kinetics of *fac*-Re(I) tricarbonyl complexes are virtually unexplored and included until recently only water exchange studies and aqua substitution kinetics of *fac*-[$Re(CO)_3(H_2O)_3]^+$.[16−18] Results obtained here indicated toward an I_d type mechanism for aqua substitution, since the rate of water exchange was similar to the substitution rates. Another interesting observation is that there seemed to be a mechanistic changeover from I_d for N donor type ligands to I_a for the softer S donor type entering ligands. This is an

Received: August 29, 2012
Published: October 22, 2012

   dx.doi.org/10.1021/ic301891u | *Inorg. Chem.* 2012, 51, 11996−12006

important prospect and provides a good reason for including mechanistic studies as part of radiopharmaceutical design. Knowing the intimate mechanism of how a radiopharmaceutical will form will enable the synthetic chemist to design optimum conditions for labeling.

The substitution of coordinated methanol by a large range of entering ligands from complexes of the type *fac*-[Re(L,L′-Bid)$(CO)_3$(MeOH)] (with L,L′-Bid = *N*,*N*′- *N*,*O*-, and *O*,*O*′-donor bidentate ligands) in methanol solvent[19] was reported recently as part of an investigation of the validity of the [2 + 1] approach adopted by Alberto. The [2 + 1] approach consists of a bidentate ligand of which the lipophilicity can be controlled and a monodentate bifunctional that can act as a potential linker to a biologically active molecule.[11,12,20] This is a versatile synthetic pathway where one can optimize the properties of the radionuclides. Unexpectedly, the kinetic results obtained here yielded a 4 orders of magnitude increase of activation for the methanol substitution, as indicated by the second-order rate constants. This was achieved by varying the bidentate ligand from *N*,*N*′-Bid (1,10-phenanthroline, 2,2′-bipyridine) to *N*,*O*-Bid (2-picolinate, 2-quinolate) to *O*,*O*′-Bid (tribromotropolonate, hydroxyflavonate; n = 0, +1). An I_d mechanism was proposed from the activation parameters. These results illustrated that the reactivity of the normally inert Re(I) metal center could be significantly manipulated and opened the door for more work in this area, especially if the [2 + 1] approach is adopted. Unfortunately, these reactions had to be performed in methanol as solvent due to solubility issues.

However, it is imperative to study the *aqueous* substitution behavior and kinetics of these types of complexes to not only fully understand the fundamental chemistry and mimic the in vivo performance more closely but also because rhenium(I) tricarbonyl complexes easily form polymers in less acidic aqueous solutions and since most labeling kits on the market utilize normal saline solution during the synthysis.

In this paper, the aqua substitution behavior and anation kinetics by thiocyanate ions of the water-soluble complex *fac*-[Re(Trop)$(CO)_3(H_2O)$], stable in water over a wide pH range, are reported as well as the corresponding comparative methanol substitution kinetics of the analogous *fac*-[Re(Trop)-$(CO)_3$(MeOH)] in methanol as solvent. Thiocyanate ion (NCS^-) was chosen as entering ligand to simplify the aqueous chemistry, since it does not form different species in solution in the pH range studied and is also present in blood plasma, thus serving as a good model of a typical "biological" ligand. In particular, this also affords the opportunity to compare the data obtained to that for the methanol substitution reaction of the methanol complex.

There are only a few crystal structure reports of *fac*-[Re$(CO)_3$(*L*,*L*′)(H_2O)] (*L*,*L*′ = two monodentate or one bidentate ligand) in the literature. For this reason, and with the aim to better understand the effect of ligand dynamics on the Re−OH_2 bond, the available solid-state data is expanded by reporting the crystal structure of *fac*-[NEt_4][Re(Trop)-$(CO)_3(H_2O)]\cdot NO_3\cdot H_2O$. Furthermore, as additional confirmation that monodentate substitution indeed takes place, the structure of the pyridine-substituted product, *fac*-[Re(Trop)-$(CO)_3$(Py)], is reported as proof of aqua substitution, while only the spectroscopic and chemical analysis of the thiocyanato complex is reported, since all attempts to isolate crystals for single crystal experiments failed.

EXPERIMENTAL SECTION

General. All chemicals and reagents used were of analytical reagent grade, purchased from Sigma-Aldrich. Double-distilled water was used in all the experiments. All the pH measurements were performed on a Hanna pH 211 Microprocessor pH meter, with an HI 1131 probe using standard buffer solutions for calibrations, with pH = $-\log[H^+]$. The kinetic measurements were performed on a Varian Cary 50 Conc UV−visible spectrophotometer or a HPSF-56 stopped-flow system, supplied by TgK Scientific. The system can operate over a temperature range from −40 to 100 °C. The dead time is less than 2 ms at 298 K. The temperature within the system was controlled and maintained at ±0.1 °C by means of a circulating water bath system, coupled to a personal computer capable of performing least-squares analyses on the absorption values vs time data obtained from the kinetic runs. Infrared spectra of the complexes were recorded on a Bruker Tensor 27 Standard System spectrophotometer and a Varian Scimitar series FT-IR with a laser range of 4000−370 cm^{-1} that is coupled to a personal computer. Samples were analyzed as KBr pellets. All ^1H and ^{13}C NMR spectra were obtained on Bruker 600 MHz or Varian 300 MHz nuclear magnetic resonance spectrometers at ambient temperature (22 ± 1 °C). Scientist Micromath, Version 2.01[21] and Microsoft Office Excel 2007[22] were used to fit the data to the specific functions. The temperature was controlled and maintained at ±0.1 °C by circulating water bath systems.

[NEt_4] fac-[Re(Trop)$(CO)_3(H_2O)]$.NO_3.H_2O (1). [NEt_4]$_2$[Re-$(CO)_3(Br)_3$] (0.1 g, 0.130 mmol) was dissolved in H_2O at pH 2.2 (adjusted with HNO_3). Silver nitrate (0.066 g, 0.389 mmol) was added to the solution and the mixture stirred for 24 h at room temperature. After the AgBr was filtered off, tropolone (0.016 g, 0.131 mmol) was added to the solution and the reaction stirred under N_2 for 48 h. The reaction mixture was filtered and the filtrate (pH = 2.5) was dried in vacuo and redissolved in water for crystallization to take place. The crystals obtained were grown by evaporation of the water from the filtrate. The product was found to be soluble in water when diluted. Yield: 0.0737 g, 92%. IR (KBr, cm^{-1}): ν_{CO} = 1879, 2006. UV/vis: λ_{max} = 272 nm, ε = 9400 M^{-1} cm^{-1}. ^1H NMR (CD_3COCD_3): δ = 2.05 (s, 12H), 2.85 (s, 8H), 7.23 (q, 1H, J = 10 Hz, 21.2 Hz), 7.40 (dd, 2H, J = 4.8 Hz, 11.2 Hz), 7.62 (t, 2H, J = 10 Hz). ^{13}C NMR (CD_3COCD_3): δ = 11.5, 52.1, 127.5, 128.0, 128.5, 139.0, 139.2, 185.3. HPLC: 18.79 min. Anal. Calcd: C, 34.89; H, 4.72; N, 4.52. Anal. Found: C, 35.01; H, 4.67; N, 4.69.

fac-[Re(Trop)$(CO)_3(H_2O)]$ (2). Compound **2** was obtained from the precipitate of **1**. IR (KBr, cm^{-1}): ν_{CO} = 1880, 2007. UV/vis: λ_{max} = 272 nm, ε = 9400 M^{-1} cm^{-1}. ^1H NMR (CD_3COCD_3): δ = 7.40 (q, 1H, J = 9.6 Hz, 20.4 Hz), 7.49 (dd, 2H, J = 4.8 Hz, 10.8 Hz), 7.66 (t, 2H, J = 9.6 Hz). ^{13}C NMR (CD_3COCD_3): δ = 127.8, 128.9, 139.4, 139.7, 185.7. HPLC: 18.70 min. Anal. Calcd: C, 29.34; H, 1.72. Anal. Found: C, 29.44; H, 1.78.

[NEt_4] fac-[Re(Trop)$(CO)_3$(NCS)] (3). Sodium thiocyanate (1 mL of a 1.95 × 10^{-2} M methanol solution) was added to *fac*-[Re(Trop)-$(CO)_3(H_2O)$] (10 mL of a 1.95 × 10^{-3} M methanol solution) and the mixture stirred at room temperature for 1 h. The product formed as a yellow precipitate and was dried in vacuo. Yield: 10.5 mg, 92%. All attempts to obtain crystals suitable for single crystal X-ray studies failed. IR (KBr, cm^{-1}): ν_{CO} = 1900, 2020, ν_{NCS} = 2151. UV/vis: λ_{max} = 268 nm, ε = 10 930 M^{-1} cm^{-1}. ^1H NMR (CD_3COCD_3): δ = 1.29 (s, 12H), 2.82 (s, 8H), 6.98 (t, 1H, J = 9.6 Hz), 7.18 (d, 2H, J = 10.8 Hz), 7.45 (t, 2H, J = 10.8 Hz). ^{13}C NMR: (CD_3COCD_3): δ = 11.2, 31.5, 50. 8, 127.4, 129.0, 138.7, 184.4. Anal. Calcd: C, 39.50; H, 4.36; N, 4.85. Anal. Found: C, 39.62; H, 4.47; N, 4.89.

fac-[Re(Trop)$(CO)_3$(Py)] (4). Pyridine (1 mL of a 1.95 × 10^{-2} M methanol solution) and *fac*-[Re(Trop)$(CO)_3(H_2O)$] (10 mL of a 1.95 × 10^{-3} M methanol solution) were stirred for 1 h at room temperature. The reaction mixture was dried in vacuo to yield the yellow product. The crystals reported were grown from a methanol solution of the product. Yield: 8.9 mg, 97%. IR (KBr, cm^{-1}): ν_{CO} = 1889, 2011. UV/vis: λ_{max} = 315 nm, ε = 9430 M^{-1} cm^{-1}. ^1H NMR (CD_3COCD_3): δ = 7.11 (t, 1H, J = 9.6 Hz), 7.33 (d, 2H, J = 10.8 Hz), 7.51 (d, 2H, J = 10.8 Hz), 7.56 (q, 2H, J = 5.4 Hz), 8.00 (tt, 1H, J = 1.8

dx.doi.org/10.1021/ic301891u | Inorg. Chem. 2012, 51, 11996−12006

Hz, 7.8 Hz), 8.58 (dd, 2H, J = 1.8 Hz, 6.6 Hz). ^{13}C NMR (CD_3COCD_3): δ = 120.9, 122.6, 124.1, 128.3, 135.9, 136.1, 137.9, 149.1, 172.6. Anal. Calcd: C, 38.30; H, 2.14; N, 2.98. Anal. Found: C, 38.51; H, 2.24; N, 3.05.

fac-[Re(Trop)(CO)$_3$(CH$_3$OH)] (5). *fac*-[Re(Trop)(CO)$_3$(H$_2$O)] (0.02 g) was dissolved in methanol and stirred for 10 min. The solution was dried and the methanol complex was isolated. Yield: 19 mg, 92%. IR (KBr, cm^{-1}): ν_{CO} = 1878, 2007. UV/vis: λ_{max} = 275 nm, ε = 8530 M^{-1} cm^{-1}. ^{1}H NMR (CD_3COCD_3): δ = 3.46 (s, 3H), 7.24 (t, 1H, J = 9.2 Hz), 7.30 (d, 2H, J = 10.2 Hz), 7.66 (t, 2H, J = 10.2 Hz). ^{13}C NMR: (CD_3COCD_3): δ = 128.6, 129.7, 139.5, 185.0. Anal. Calcd: C, 31.20; H, 2.14. Anal. Found: C, 31.12; H, 2.05.

X-ray Structure Determinations. Diffraction data for *fac*-[NEt$_4$][Re(Trop)(CO)$_3$(H$_2$O)]·NO$_3$·H$_2$O (**1**) and *fac*-[Re(Trop)(CO)$_3$(Py)] (**2**) are presented in Table 1. **1** was collected at 183(2) K on an Oxford Diffraction Xcalibur system with a Ruby detector using Mo Kα radiation (λ = 0.7107 Å) that was graphite-monochromated. The program suite CrysAlis^{Pro} [23] was used for data collection, multiscan absorption correction, and data reduction. **2** was collected at 100 K on a Bruker X8 ApexII 4K diffractometer using monochromated Mo Kα radiation (λ = 0.710 73 Å). The cell parameters were refined by the SAINT-Plus[24] program while SADABS[25] was used for the absorption corrections. Suitable crystals were covered with oil (Infineum V8512, formerly known as Paratone N), mounted on top of a glass fiber, and immediately transferred to the diffractometer. Structures were solved with direct methods using SIR97[26] and were refined by full-matrix least-squares methods on F^2 with SHELXL-97[27] and WinGX.[28] The structure was checked for higher symmetry with the help of the program Platon.[29] The molecular graphics were obtained with DIAMOND.[30] Aromatic hydrogen atoms were placed in geometrically idealized positions (C−H = 0.95 Å) and constrained to ride on their parent atoms with U_{iso}(H) = 1.2U_{eq}(C). Methyl and methene hydrogen atoms were placed in geometrically idealized positions (C−H = 0.98 Å and 0.99 Å, respectively) and constrained to ride on their parent atoms with U_{iso}(H) = 1.5U_{eq}(C). Aqua hydrogen atoms were located from Fourier difference maps and constrained with equal O−H distances [0.85(2) Å].

Table 1. Crystallographic Data of *fac*-[NEt$_4$][Re(Trop)(CO)$_3$(H$_2$O)]·NO$_3$·H$_2$O (1) and *fac*-[Re(Trop)(CO)$_3$(Py)] (4)

empirical formula	$C_{28}H_{34}N_2O_{17}Re$ (**1**)	$C_{15}H_{10}NO_5Re$ (**4**)
formula weight (g mol^{-1})	1042.99	470.45
crystal system	monoclinic	monoclinic
space group	$P2_1/c$	$P2_1/c$
a (Å)	14.5451(7)	16.349(5)
b (Å)	10.3208(4)	6.890(5)
c (Å)	11.6301(4)	14.239(5)
α (deg)	90.00	90.000(5)
β (deg)	90.372(4)	114.390(5)
γ (deg)	90.00	90.000(50
volume (A^3)	1744.34(12)	1460.8(13)
Z	2	4
ρ_{calc} (g cm^{-3})	1.986	2.139
crystal color	yellow	yellow
crystal morphology	cuboid	needle
crystal size (mm)	0.11 × 0.08 × 0.05	0.18 × 0.06 × 0.03
μ (mm^{-1})	7.010	8.341
F(000)	1004.0	888.0
θ range (deg)	2.63−30.82	3.26−28.20
Index ranges	$-19 \le h \le 1$	$-21 \le h \le 19$
	$-9 \le k \le 1$	$-9 \le k \le 9$
	$-15 \le l \le 11$	$-14 \le l \le 18$
reflections collected	9950	20542
unique reflections	4500	3635
reflections with $I > 2\sigma(I)$	3316	2983
R_{int}	0.0505	0.0437
completeness to 2θ (°, %)	28.70, 99.6	28.31, 99.3
data/restraints/parameters	4500/5/280	3635/0/199
GooF	1.063	1.189
R [$I > 2\sigma(I)$]	R_1 = 0.053	R_1 = 0.0228
	wR$_2$ = 0.1001	wR$_2$ = 0.0577
R (all data)	R_1 = 0.0866	R_1 = 0.0347
	wR$_2$ = 0.1086	wR$_2$ = 0.0858
ρ_{max}, ρ_{min} (e A^{-3})	2.386, −2.611	1.074, −1.325

The diffraction images of **1** were integrated as a nonmerohedral twin (ratio 89:11).[31] The two components are related by a 20.92° rotation around *hkl* 0.9980 0.0624 −0.0081. In the refinement, only the major component was considered.

Kinetic Studies. The kinetic reactions were measured aerobically under pseudo-first-order conditions. The ligand was in excess in each case and the metal concentration was kept constant. The ionic strength of the aqueous solutions was maintained at 1 M by using NaClO$_4$. Each kinetic run was performed at least twice and an average of the values was used. In the figures presented, the solid lines represent the computer least-squares fits of the data, while the single points represent the experimental values, denoted by selected symbols. The rates and concentration dependences obtained in this study assumes that the aqua complex, *fac*-[Re(Trop)(CO)$_3$(H$_2$O)], with TropH = tropolone, immediately upon dissolution in methanol exchanges the coordinated aqua to form the corresponding methanol complex, *fac*-[Re(Trop)(CO)$_3$(MeOH)].[17,32]

In all the calculations, pH = −log[H$^+$]. The Beer−Lambert law, with incorporation to the well-known first-order exponential, yields eq 1 for the evaluation of the absorbance change vs time data in simple first-order reactions.

$$A_t = A_\infty - (A_\infty - A_0)e^{-k_{obs}t} \quad (1)$$

The substitution of the coordinated aqua/methanol by NCS$^-$ ions was performed at four temperatures under pseudo-first-order conditions and with the thiocyanate ion concentration varying between 2.5 × 10^{-3} and 3 × 10^{-2} M and between 2.0 × 10^{-2} and 2.0 × 10^{-1} M for the aqua and methanol substitution, respectively.

The pseudo-first-order rate constant (k_{obs}) is determined by a least-squares fit of the absorbance vs time data for the reaction. This equation was used in all the kinetic runs. The concentration dependence of k_{obs} for the substitution process of the aqua and methanol ligand by thiocyanate ions (NCS$^-$) in *fac*-[Re(Trop)(CO)$_3$(H$_2$O)] and *fac*-[Re(Trop)(CO)$_3$(MeOH)] respectively, is given by eq 2.

$$k_{obs} = k_1[NCS^-] + k_{-1} \quad (2)$$

Equilibrium Studies. The aqua and methanol substitution in *fac*-[Re(Trop)(CO)$_3$(H$_2$O)] and *fac*-[Re(Trop)(CO)$_3$(MeOH)], respectively, by thiocyanate ions can be studied as pseudo-first-order processes defined by Schemes 1 and 2, respectively. For this study, it was assumed that the thiocyanate ligand coordinates with the nitrogen atom; therefore, it is written as NCS$^-$.

The acid dissociation constant of *fac*-[Re(Trop)(CO)$_3$(H$_2$O)] was determined spectrophotometrically at 25.0 °C and at 275 nm by adjusting the pH of a 1 × 10^{-4} M *fac*-[Re(Trop)(CO)$_3$(H$_2$O)] solution from pH 7 to 11 with sodium hydroxide (aqueous solutions from 1 × 10^{-6} to 1 × 10^{-2} M from a 1.0 M stock solution) and measuring the absorbance each time over a 3 h period.

The equilibrium constants, K_1, were determined kinetically throughout this study by means of $K_1 = k_1/k_{-1}$. The rate constants k_1 and k_{-1}, are calculated from a graph of k_{obs} vs [X], which yields a straight line with k_{-1} as the intercept and k_1 as the slope. Only one reaction, for both the aqua substitution and methanol substitution reactions, was observed spectroscopically, indicating a one-step process for both the aqua and methanol complexes with NCS$^-$ ions. K_1 was

Scheme 1. Schematic Representation of the Aqueous Protonation and Aqua Substitution of *fac*-[Re(Trop)(CO)$_3$(H$_2$O)] by NCS$^-$ Ions

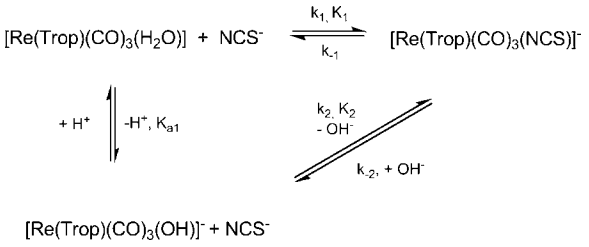

Scheme 2. Simplified Mechanism for the Methanol Substitution Reaction between *fac*-[Re(Trop)(CO)$_3$(MeOH)] and NCS$^-$ Ions

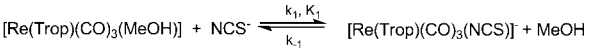

also determined spectrophotometrically under equilibrium conditions from a plot of Abs vs [NCS$^-$] and by using eq 3.

$$\text{Abs} = (A_0 + A_1K_1[\text{L}])/(1 + K[\text{L}]) \quad (3)$$

RESULTS AND DISCUSSION

Synthesis. All the spectroscopic results, together with the results obtained from elemental analysis and X-ray diffraction, indicate successful synthesis. It is interesting to note that we were unable to obtain crystals suitable for X-ray diffraction of *fac*-[Re(Trop)(CO)$_3$(H$_2$O)] alone and that successful crystallization only occurred in the presence of tetraethylammonium and nitrate ions. Also, *fac*-[Re(Trop)(CO)$_3$(H$_2$O)] in MeOH solvates easily to form *fac*-[Re(Trop)(CO)$_3$(MeOH)], as indicated by elemental analysis. This result is similar to that obtained in our previous work.[19,29]

X-ray Crystallography. The X-ray crystal data of **1** and **2** and selected bond angles and lengths are represented in Tables 1 and 2, respectively. The molecular structures of **1** and **2** are shown in Figure 1 with the corresponding numbering scheme and with the hydrogen atoms, cation, anion, and solvate water molecule omitted for clarity. For the sake of brevity and uniformity, the plane formed by the two carbonyl ligands trans to the bidentate ligand and the ligand itself, will be referred to throughout as the equatorial plane. The two ligands on either side of the equatorial plane in the apical positions will be referred to as axial ligands.

The diffraction images of *fac*-[NEt$_4$][Re(Trop)(CO)$_3$(H$_2$O)]·NO$_3$·H$_2$O were integrated as a nonmerohedral twin (ratio 89:11).[33] The two components are related by a 20.92° rotation around *hkl* 0.9980 0.0624 −0.0081. In the refinement, only the major component was considered. N1, of the nitrate anion, and N2, of the tetraethylammonium cation, are located on inversion centers, and the nitrate and tetraethylammonium ions exhibit a positional disorder in a 0.5:0.5 ratio as required by the inversion centers. Due to the disorder in this structure, the positions of the protons on the coordinated aqua could not be determined reliably and are therefore not reported. Some selected bond distances and angles of **1** and **2** are reported in Table 2 with the data of the bromido analogue, *fac*-[NEt$_4$][Re(Trop)(CO)$_3$(Br)],[34] included for comparison while the molecular diagrams of **1** and **2** are given in Figure 1.

The asymmetric unit in **1** consists of a neutral *fac*-[Re(Trop)(CO)$_3$(H$_2$O)] molecule, a nitrate anion, tetraethylammonium cation, and a solvate water molecule. The Re(I) atom in **1** is coordinated by three facially arranged carbonyl ligands, an aqua ligand, and the tropolonato bidentate ligand. In the structure of **1**, the Re(I) atom displays a distorted octahedral environment with the angles in the coordination polyhedron ranging from 74.82(17)° for the bite angle O11−Re−O12 to 92.7(3)° for C1−Re−O4. The O4−Re−C3 angle of 176.8(2)° deviates significantly from 180°. Similar distortion of the octahedral geometry is also reported in **2** and *fac*-[Re(Trop)(CO)$_3$(Br)]$^-$, with the angles reported in Table 2.

fac-[Re(Trop)(CO)$_3$(Py)] (**2**) crystallized in the monoclinic $P2_1/c$ space group, with one molecule in the asymmetric unit. The Re(I) center is coordinated by three facial carbonyl ligands, a tropolonato bidentate ligand, and a pyridine ligand coordinated in the 6-position.

The rhenium to carbonyl ligand distances in the structures of **1** and **2** are within normal range.[5,19,34,43,35] The rhenium−tropolonato distances (Re−O11 and Re−O12) of 2.121(5) and 2.108(4) Å for **1** and 2.121(4) and 2.136(3) Å for **2** correspond well with that of *fac*-[NEt$_4$][Re(Trop)(CO)$_3$Br] and other similar structures.[36,37]

The O11−Re1−O12 bite angles of the tropolonato ligand of 74.82(17)° and 74.68(14)° for **1** and **2**, respectively, also compare well to other *O*,*O*′-Bid-type complexes,[34,36,37] while

Table 2. Selected Bond Distances and Angles for *fac*-[NEt$_4$][Re(Trop)(CO)$_3$(H$_2$O)]·NO$_3$·H$_2$O (1), *fac*-[Re(Trop)(CO)$_3$(Py)] (2), and *fac*-[NEt$_4$][Re(Trop)(CO)$_3$(Br)][34]

	1	2	*fac*-[NEt$_4$][Re(Trop)(CO)$_3$(Br)]
Re−CO range	1.886(8)−1.894(8)	1.898(5)−1.930(6)	1.861(7)−1.923(18)[a]
Re−O11	2.121(5)	2.121(4)	2.126(3)
Re−O12	2.108(4)	2.136(3)	2.135(3)
Re−X	2.213(5) (O4)	2.208(4) (N1)	2.467(16)/2.6334(9)[a] (Br)
O11−Re−O12	74.82(17)	74.68(14)	74.88(12)
X−Re−C3	176.8(2)	177.55(18)	175.61(19)/171.5(19)
X−Re−O11	79.5(2)	81.66(15)	86.3(3)/82.07(9)
C1−Re−C2	87.3(4)	87.3(2)	87.6(2)
C1−Re−C3 C2−Re−C3	85.6(3)	86.9(2)	92.1(19), 87.7(2)
C1−Re−X	92.7(3)	93.9(2)	95.6(3), 95.34(14)
C2−Re−X	96.2(3)	91.8(2)	94.80(15), 96.0(3)

[a]Substitutional disordered carbonyl and bromido ligand in a 0.92:0.08 ratio.

dx.doi.org/10.1021/ic301891u | *Inorg. Chem.* 2012, 51, 11996−12006

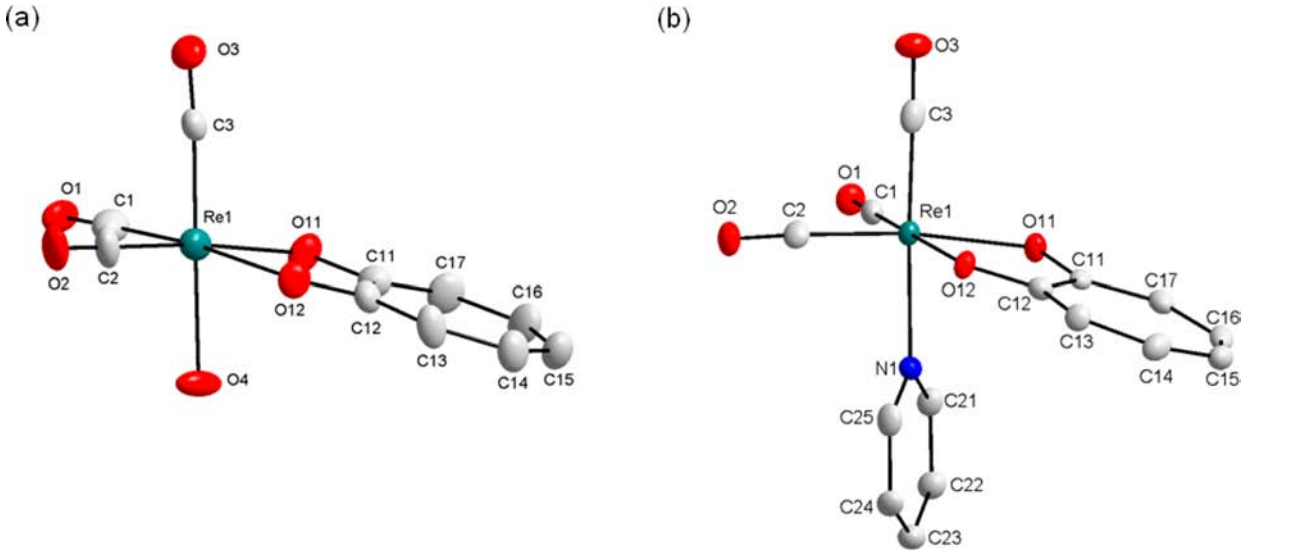

Figure 1. Molecular diagram of *fac*-[NEt_4[Re(Trop)$(CO)_3(H_2O)$]·NO_3·H_2O (a) and *fac*-[Re(Trop)$(CO)_3$(Py)] (b). Hydrogen atoms, counterions, and the water solvent molecule are omitted for clarity.

the axial Re1−N1 distance of 2.208(4) Å is in good agreement with other rhenium(I)−pyridine distances.[38−40] The Re−OH_2 distance of 2.213(5) Å is of most importance here and compares well with the 2.170(5) Å obtained for the tribromotropolonato complex *fac*-[Re$(TropBr_3)$-$(CO)_3(H_2O)$]·CH_3OH, but is slightly shorter than the Re−O distance in *fac*-[Re$(CO)_3(H_2O)_3]^+$ [2.201(14) Å].[41] These two examples are the only two of a *fac*-[Re(*O*,*O*′-Bid)-$(CO)_3(OH_2)$] (*O*,*O*′-Bid = oxygen, oxygen bidentate ligand) known.[42] It compares quite well with the 2.142(7) Å in the *trans*-[$ReO(OH_2)(CN)_4]^-$ complex[43,44] and the 2.165(5) Å in $[Re(NO)(H_2O)(CN)_4]^{2-}$ but is, as expected, shorter than the 1.90(1) Å reported for *trans*-[$ReO(OH)(CN)_4]^{2-}$.[45,46]

The planarity of the tropolonato ring system, O11−O12−C11−C12−C13−C14−C15−C16−C17, is illustrated by the small deviations from the plane through these atoms, with the largest deviation being 0.021(6) Å for C17 in **1** and 0.042(4) Å for C16 in **2**.

The structure of **1** exhibits an extensive hydrogen-bonding network (see Supporting Information) with the solvent molecules and the cocrystallizing nitrate and tetraethylammonium ions. Two intramolecular (O−H···O) and six intermolecular hydrogen bonds (C−H···O and O−H···O) are observed. The rhenium(I) units pack in alternating orientations along the *a*,*b*-plane, in a head-to-head fashion. Three C−H···O hydrogen bonds are observed in the crystal structure of *fac*-[Re(Trop)$(CO)_3$(Py)]. All three of these hydrogen bonds are intermolecular bonds from the coordinated pyridine ring. The molecules pack in a head-to-head fashion, in alternating "columns", along the *a*-axis.

Spectroscopy. All the synthesized complexes exhibit typical UV−vis spectra of low spin d^6 metal Re(I) under the influence of the strong ligand field affected by the *fac*-tricarbonyl orientation, and once ligand substitution has been affected, typical UV−vis transitions are observed.[47]

The IR data as reported in the Experimental Section indicate that the symmetric stretching bands fall in the same range as observed for the similar bromotropolonato and hydroxyflavonato complexes (2020 cm^{-1} compared to 2022 and 2013 cm^{-1}, respectively).[19] This is an indication of the electron density on the metal center due to the influence of the bidentate ligand as described previously and will be discussed further in later paragraphs.[19,48−51]

Equilibrium Studies. Previous studies have shown that 3-hydroxyflavone, as *O*,*O*′-Bid ligand, is able to significantly activate the normally inert rhenium(I) metal center.[19] If one considers the transition from the pure *fac*-[Re$(CO)_3(H_2O)_3]^+$ complex, an activation of more than 5 orders of magnitude (ca. 4×10^5) was observed for the methanol substitution reactions of *fac*-[Re(Flav)$(CO)_3$(MeOH)] (with FlavH = 3-hydroxyflavone).

In the first part of this section, the influence of H^+ ions on the reactivity of *fac*-[Re(Trop)$(CO)_3(H_2O)$] toward aqua substitution with NCS^- ions is reported (Scheme 1).

The thermodynamic pH dependence of *fac*-[Re(Trop)-$(CO)_3(H_2O)$] was studied at 25.0 °C in the pH range 7−11. In general, the acid/base behavior of the monoprotic Bronsted acid *fac*-[Re(Trop)$(CO)_3(H_2O)$], which dissociates to *fac*-[Re(Trop)$(CO)_3(OH)]^-$, is shown in Scheme 1. Equation 4 incorporates Beer's law to allow for the determination of the acid dissociation constant, where Abs = observed absorbance at a specific pH; A_h = the absorbance of the protonated species, *fac*-[Re(Trop)$(CO)_3(H_2O)$]; A_0 = the absorbance of the deprotonated species, *fac*-[Re(Trop)$(CO)_3(OH)]^-$; and K_{a1} = the acid dissociation constant.

$$\text{Abs} = \frac{A_h + A_0(K_{a1}/[H^+])}{1 + (K_{a1}/[H^+])} \quad (4)$$

The pK_{a1} value shown in Scheme 2 was determined as 8.96 ± 0.02 (Figure 2a) from a nonlinear fit of the data to eq 4. Egli et al.[52] studied the hydrolysis of the *fac*-[Re$(CO)_3(H_2O)_3]^+$ aqua ion and found the pK_{a1} and pK_{a2} values of the mononuclear *fac*-[Re$(CO)_3(H_2O)_3]^+$ species, yielding the deprotonation products *fac*-[Re$(CO)_3(H_2O)_2(OH)$] and *fac*-[Re$(CO)_3(H_2O)$-$(OH)_2]^-$ to be 7.5 ± 0.2 and 9.3 ± 0.3, respectively.

The substitution of the coordinated aqua/hydroxido from *fac*-[Re(Trop)$(CO)_3(H_2O)$] and *fac*-[Re(Trop)$(CO)_3(OH)^-$] (see Scheme 1) by thiocyanate ions was studied kinetically between pH 6.3 and 10.0. In principal, both these species can react with NCS^- ions so that the rate law given in eq 5 can be derived from Scheme 1.[45] For this study, it was assumed that

dx.doi.org/10.1021/ic301891u | *Inorg. Chem.* 2012, 51, 11996−12006

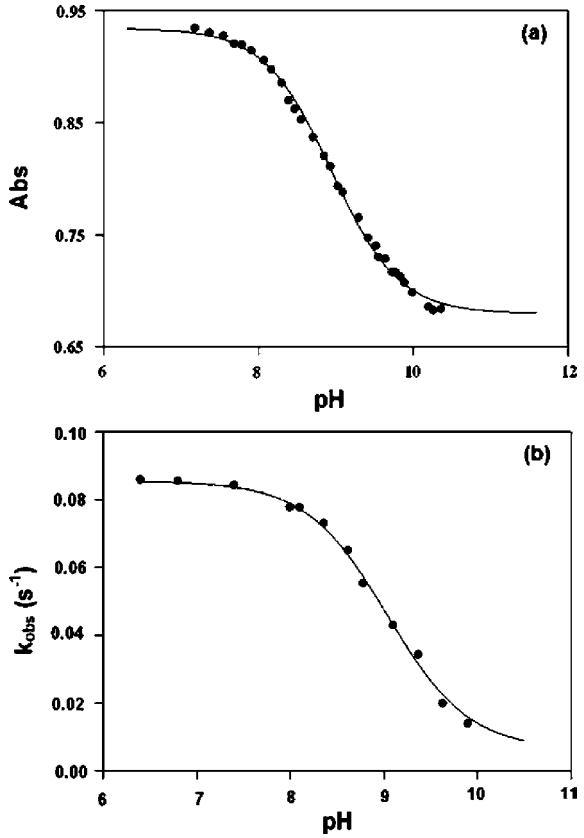

Figure 2. Plots of (a) absorbance vs pH data for *fac*-[Re(Trop)-$(CO)_3(H_2O)$] for the determination of pK_{a1}. [Re] = 1×10^{-4} M, 25.0 °C, λ = 275 nm, μ = 1 M ($NaClO_4$). Data fitted to eq 4. (b) Plot of k_{obs} vs pH for the reaction between *fac*-[Re(Trop)$(CO)_3(H_2O)$] and NCS^- ions. [Re] = 5×10^{-5} M, [NCS^-] = 3×10^{-2} M, λ = 260 nm, 25.0 °C, μ = 1 M ($NaClO_4$). Data fitted to eq 6.

the thiocyanate ligand coordinates with the nitrogen atom;l therefore, it is written as NCS^-.

$$k_{obs} = \left(\frac{k_1[H^+] + k_2K_{a1}}{K_{a1} + [H^+]}\right)[NCS^-] + k_{-1} + k_{-2}[OH^-] \quad (5)$$

The proposed mechanism in Scheme 1 was verified by several preliminary experiments. First, the stability of *fac*-[Re(Trop)$(CO)_3(H_2O)$]/*fac*-[Re(Trop)$(CO)_3(OH)^-$] with increasing pH was monitored by slowly increasing the pH of a 1×10^{-4} M solution of the rhenium complex. Slow changes in the spectrum were observed at pH >10.0. From this, it was confirmed that it is most likely due to the formation of dinuclear/polymeric Re(I) species.[52] Figure 3 illustrates the change in the UV/vis spectrum for a 1×10^{-4} M *fac*-[Re(Trop)$(CO)_3(H_2O)$] solution. Spectrum 1 in Figure 3 represents the solution at pH 6.4. The pH was increased to pH 9.5, yielding the spectrum illustrated by spectrum 2 in Figure 3, indicating the formation of *fac*-[Re(Trop)$(CO)_3(OH)^-$].

The pH was then also further increased to 10.1, as shown by spectrum 3 in Figure 3, where the formation of the Re(I) dimer $[Re_2(CO)_6(\mu_2\text{-}OH)_3]^-$ is proposed, with the definite peak at 297 nm.[39] When the pH of the same solution is lowered to 6.3, the peak at 297 nm disappears and a spectrum virtually identical to that obtained at pH 6.4 is observed, indicating that the *fac*-[Re(Trop)$(CO)_3(H_2O)$] species is once again formed. This confirmed that the reaction is reversible.

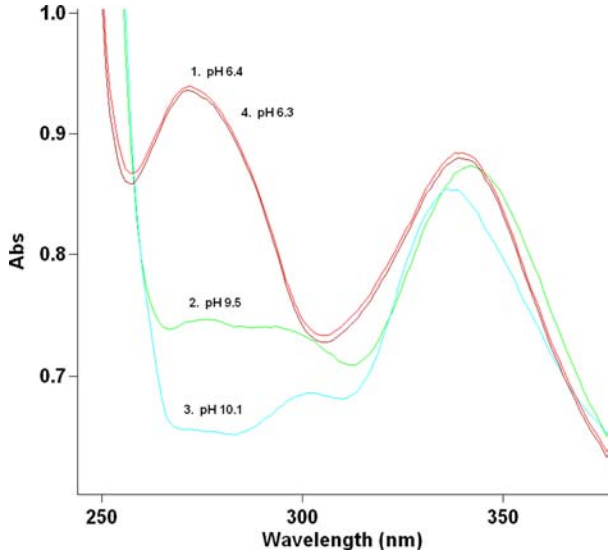

Figure 3. UV/vis spectral changes as a function of pH of *fac*-[Re(Trop)$(CO)_3(H_2O)$] at pH 6.4 and pH 6.3, *fac*-[Re(Trop)-$(CO)_3(OH)]^-$ at pH 9.5, and the Re(I) dimeric species at pH 10.1. [Re] = 1×10^{-4} M, μ = 1 M ($NaClO_4$), t = 180 min.

Aqua Substitution Kinetic Study. Preliminary substitution kinetic experiments indicated that the observed rate, k_{obs}, decreases with an increase in pH. At pH ~10, the slow polymerization reactions, already mentioned, were the only reactions observed. This indicates that *fac*-[Re(Trop)-$(CO)_3(OH)^-$] does not react with NCS^- ions and that the k_2/k_{-2} pathway in Scheme 1 does not contribute significantly to the overall process, if at all, and can be ignored. A typical spectrum change of absorbance over time for the substitution reaction of *fac*-[Re(Trop)$(CO)_3(H_2O)$] with NCS^- ions is illustrated in Figure 4. Only one reaction step was observed between pH 6 and 10, which is further supporting evidence for the proposed rate law. Yet additional evidence was obtained when the reaction products from the kinetic runs were isolated from the solutions and successfully compared to the IR, UV–vis, and NMR data with that of *fac*-[NEt_4][Re(Trop)-$(CO)_3(NCS)$] (**3**).

In order to further verify the proposed mechanism, the reaction between *fac*-[Re(Trop)$(CO)_3(H_2O)$] and NCS^- ions was monitored at different pH values (Figure 2b), with μ = 1 M ($NaClO_4$) and at 25.0 °C. This data was fitted simultaneously with the data obtained at pH 6.4 (T = 25.0 °C), and values for k_1, k_{-1} and pK_{a1} were obtained from least-squares linear fits to eq 6. This is illustrated in Figure 2b. The values obtained for k_1, k_{-1}, and pK_{a1} are 2.64 ± 0.04 M^{-1} s^{-1}, 0.0063 ± 0.0009 s^{-1}, and 9.04 ± 0.02, respectively, and compare well with the data obtained before. Thus, we conclude that Scheme 1 is a fair representation of the mechanism of the aqua substitution reaction between *fac*-[Re(Trop)$(CO)_3(H_2O)$] and NCS^- ions. A summary of the data is given in Table 3.

Similar behavior was observed upon replacing NCS^- ions with pyridine as entering ligand. However, in this case, crystals suitable for X-ray crystallographic analysis were obtained, which was not the case with the thiocyanate, and the monosubstituted product was therefore additionally confirmed by the single crystal X-ray study, as reported above.

Taking into consideration that the k_2/k_{-2} pathways do not occur at the pH range studied, from the above information, and that at pH 6.4 $K_{a1} \ll [H^+]$, eq 6 simplifies to eq 2, given before.

dx.doi.org/10.1021/ic301891u | *Inorg. Chem.* 2012, 51, 11996–12006

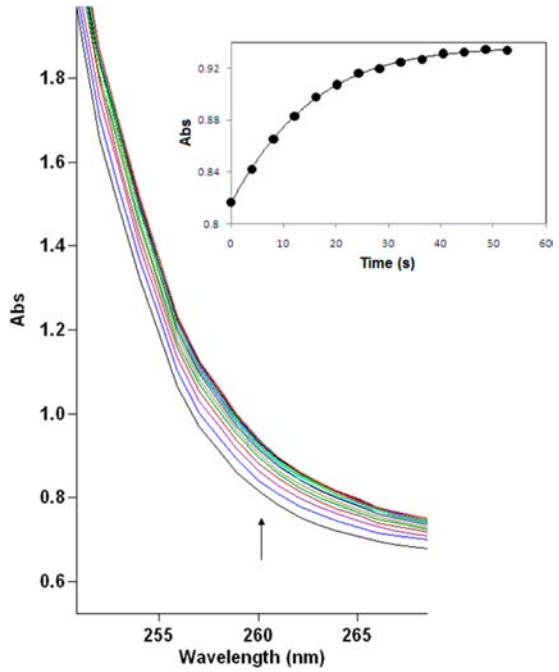

Figure 4. UV/vis absorbance change for the aqua substitution from *fac*-[Re(Trop)$(CO)_3(H_2O)$] by NCS^- ions. The absorbance vs time plot (inset) indicates only one first-order reaction. [Re] = 5×10^{-5} M, [NCS^-] = 2.5×10^{-2} M, pH 6.4, 25.0 °C, λ = 260 nm, Δt = 4 s.

$$k_{obs} = \frac{k_1[H^+][NCS^-]}{K_{a1} + [H^+]} + k_{-1} \quad (6)$$

The rate constants for all the substitution reactions between *fac*-[Re(Trop)$(CO)_3(H_2O)$] and NCS^- ions, at pH 6.4 and μ = 1 M $NaClO_4$, were calculated with the use of eq 2. The k_1 and k_{-1} values were obtained from least-squares fits of the data to eq 2, at 15.0, 25.0, 35.0, and 45.0 °C and are summarized in Table 3. The plot of k_{obs} vs [NCS^-] obtained from these fits is illustrated in Figure 5a.

The stability constant for the reaction of *fac*-[Re(Trop)$(CO)_3(H_2O)$] with NCS^- ions, K_1, was also determined spectrophotometrically by using absorbance changes induced as a function of entering ligand concentration, and the Abs vs [NCS^-] data were fitted to eq 3 as illustrated in Figure 6a. The value obtained for K_1 from this was 207 ± 14 M^{-1} and compares well to that of 330 ± 22 M^{-1} for the kinetically determined stability constant.

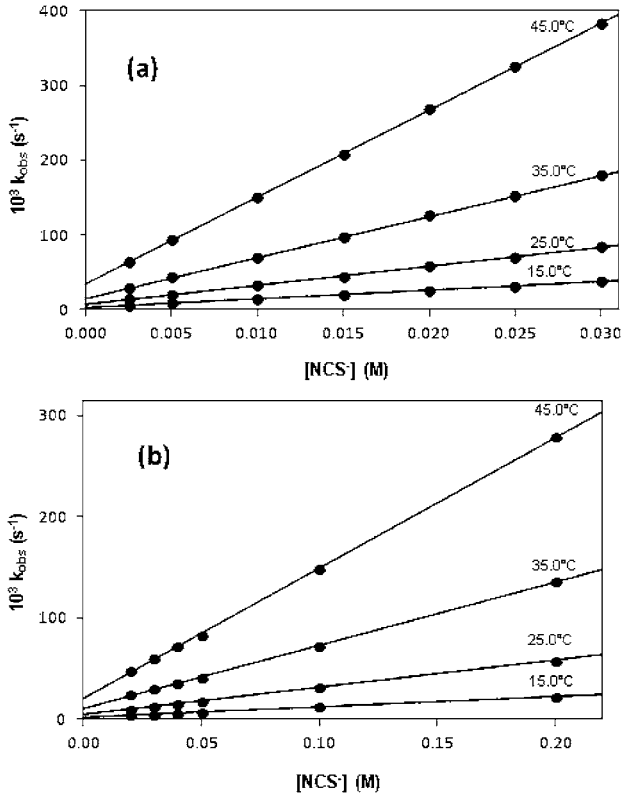

Figure 5. Plot of (a) k_{obs} vs [NCS^-] for the aqua substitution from *fac*-[Re(Trop)$(CO)_3(H_2O)$] by NCS^- ions at different temperatures. [Re] = 5×10^{-5} M, pH 6.4, λ = 260 nm, μ = 1 M ($NaClO_4$). (b) k_{obs} vs [NCS^-] for the methanol substitution from *fac*-[Re(Trop)$(CO)_3$(MeOH)] by NCS^- ions at different temperatures. [Re] = 1.0×10^{-4} M, [NCS^-] = (2.0×10^{-2})–(2.0×10^{-1}) M, λ = 265 nm, MeOH.

The activation parameters for this reaction were obtained by means of the Eyring equation[53] and yielded values of 56.1 ± 0.7 kJ mol^{-1} for $\Delta H^{\ddagger}$ and −49 ± 2 J K^{-1} mol^{-1} for $\Delta S^{\ddagger}$, as reported in Table 3. It is also clear from Table 3 that a global fit of the kinetic data yields activation parameters that are in excellent agreement with that determined from the second order rate constant fit to the Eyring equation.

Methanol Substitution Kinetic Study. The methanol substitution reactions between *fac*-[Re(Trop)$(CO)_3$(MeOH)] and NCS^- ions were monitored in methanol as solvent. The stabilities of the complex and the NCS^- ions were tested in

Table 3. Rate Constants and Activation Parameters for the Reaction between *fac*-[Re(Trop)$(CO)_3(H_2O)$] and NCS^- Ions in Water[a]

constant	15.0 °C	25.0 °C[b]	25.0 °C[c]	35.0 °C	45.0 °C
k_1 (M^{-1} s^{-1})	1.152 ± 0.004	2.54 ± 0.03	2.64 ± 0.04	5.48 ± 0.03	11.61 ± 0.02
k_{-1} (s^{-1})	0.00332 ± 0.00007	0.0077 ± 0.0005	0.0063 ± 0.0009	0.0162 ± 0.0005	0.0353 ± 0.0003
K_1 (M^{-1})	347 ± 7	330 ± 22[d]	207 ± 14[e]	338 ± 11	329 ± 3
$\Delta H^{\ddagger}_{k1}$ (kJ mol^{-1})	56.1 ± 0.7	57.9 ± 0.6[f]			
$\Delta S^{\ddagger}_{k1}$ (J K^{-1} mol^{-1})	−49 ± 2	−44 ± 2[f]			
$\Delta H^{\ddagger}_{k-1}$ (kJ mol^{-1})	57.2 ± 0.8	58 ± 3[f]			
$\Delta S^{\ddagger}_{k-1}$ (J K^{-1} mol^{-1})	−94 ± 3	−91 ± 9[f]			
pK_{a1}	8.96 ± 0.02	9.04 ± 0.02			

[a][Re] = 5×10^{-5} M, [NCS^-] = (2.5×10^{-3})–(3×10^{-2}) M, pH 6.4, λ = 260 nm, μ = 1 M ($NaClO_4$). [b]Calculated at pH 6.4 from eq 2. [c]Calculated from eq 6. [d]Calculated from $K_1 = k_1/k_{-1}$. [e]Spectrophotometrically determined from Abs vs [NCS^-] data (eq 3; Figure 6a), 25.0 °C, pH 6.4, μ = 1 M ($NaClO_4$). [f]Obtained from global fit of the data reported in Figure 5b.

dx.doi.org/10.1021/ic301891u | *Inorg. Chem.* 2012, 51, 11996–12006

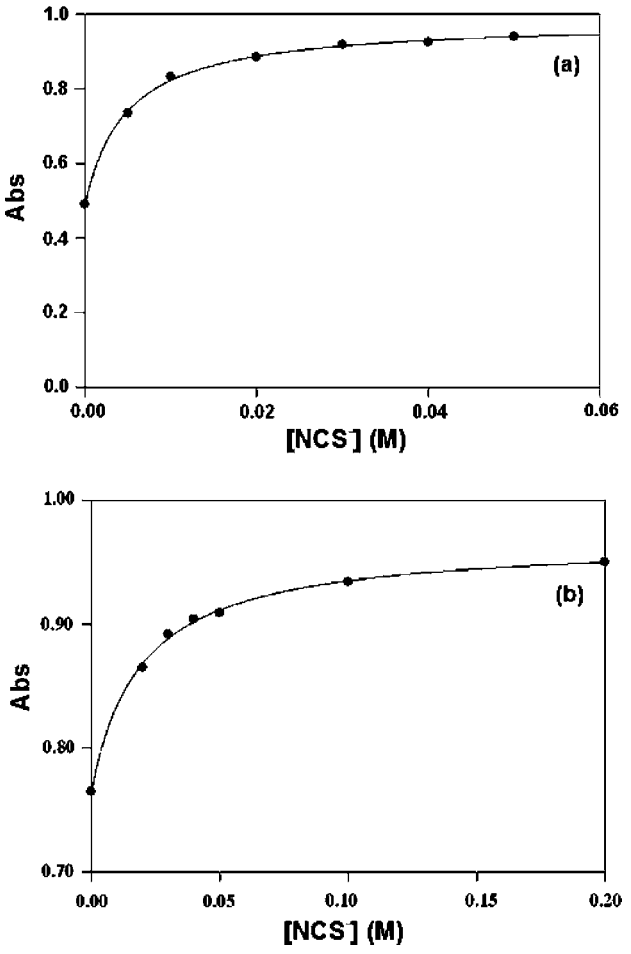

Figure 6. Determination of K_1 for (a) the aqua substitution reaction between *fac*-[Re(Trop)$(CO)_3(H_2O)$] and NCS^- ions in water from the UV/vis spectral change observed vs $[NCS^-]$. [Re] = 5.0×10^{-5} M, 25.0 °C, H_2O pH 6.4, μ = 1.0 M ($NaClO_4$), λ = 260 nm. (b) The methanol substitution reaction between *fac*-[Re(Trop)-$(CO)_3$(MeOH)] and NCS^- ions in methanol from the UV/vis spectral change observed vs $[NCS^-]$. [Re] = 1.0×10^{-4} M, 25.0 °C, λ = 275 nm.

methanol and were found to be stable for several days by monitoring appropriate solutions by UV/vis spectroscopy. A plot of k_{obs} vs $[NCS^-]$ for the reaction at four different temperatures is provided in Figure 5b. By again fitting the k_{obs} vs $[NCS^-]$ data to eq 2, the appropriate rate constants were obtained, as reported in Table 4.

The stability constant, K_1, for the methanol substitution from *fac*-[Re(Trop)$(CO)_3$(MeOH)] by NCS^- ions was obtained by fitting the absorbance change observed vs $[NCS^-]$ as described above and illustrated in Figure 6b. The value of 52 ± 4 M^{-1} for K_1, determined from the Abs vs $[NCS^-]$ data, compare well to that of 61 ± 3 M^{-1} for the kinetically determined stability constant.

The Eyring equation was subsequently used to fit the rate constants for the methanol substitution reactions (see Figure 7), and the respective activation parameters were obtained, as summarized in Table 4. The enthalpy change of activation, $\Delta H^{\ddagger}_{k1}$, was calculated as 62 ± 2 kJ mol^{-1} and the entropy change of activation, $\Delta S^{\ddagger}_{k1}$, as −48 ± 6 J K^{-1} mol^{-1}. It is clear that, as for the water substitution reported above, a global fit of the kinetic data yields activation parameters that are in excellent agreement with that determined from the second-order rate constant fit to the Eyring equation.

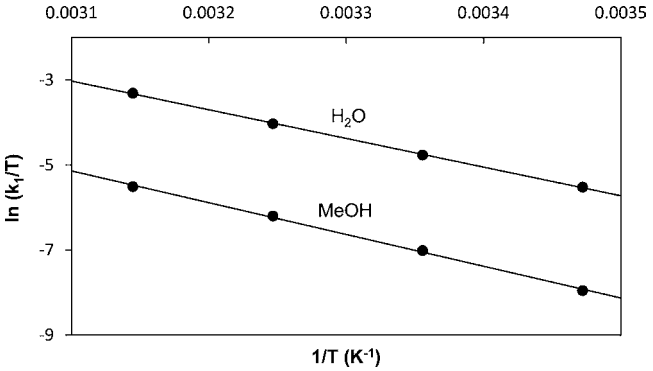

Figure 7. Eyring plot of $\ln(k_1/T)$ vs $1/T$ for the reactions between *fac*-[Re(Trop)$(CO)_3(H_2O)$] (designated H_2O) and *fac*-[Re(Trop)-$(CO)_3$(MeOH)] (designated MeOH) with NCS^- ions for a temperature range of 15.0−45.0 °C.

The activation entropy for both of the substitution of aqua/methanol from the tropolonato complex indicate fairly small negative values, indicative of an associative activation and similar to other bidentate ligand systems (see Table 6).

One of the main aims of the study of these *fac*-tricarbonyl radiopharmaceutical synthons was to synthesize a complex that is water-soluble, to be able to mimic the possible situation of

Table 4. Summary of the Rate Constants and Activation Parameters of the Reaction between *fac*-[Re(Trop)$(CO)_3$(MeOH)] and NCS^- Ions in Methanol at Different Temperatures[a]

constant	15.0 °C	25.0 °C	35.0 °C	45.0 °C
k_1 (M^{-1} s^{-1})	0.101 ± 0.001	0.268 ± 0.002	0.625 ± 0.006	1.29 ± 0.01
10^3k_{-1} (s^{-1})	2.0 ± 0.1	4.4 ± 0.2	10.5 ± 0.6	20.9 ± 0.9
K_1 (M^{-1})	51 ± 3	61 ± 3, 52 ± 4[b]	60 ± 3	62 ± 3
$\Delta H^{\ddagger}_{k1}$ (kJ mol^{-1})	62 ± 2 (58 ± 1)[c]			
$\Delta S^{\ddagger}_{k1}$ (J K^{-1} mol^{-1})	−48 ± 6 (−60 ± 3)[c]			
$\Delta H^{\ddagger}_{k-1}$ (kJ mol^{-1})	58 ± 1 (57 ± 6)[c]			
$\Delta S^{\ddagger}_{k-1}$ (J K^{-1} mol^{-1})	−95 ± 5 (−99 ± 20)[c]			

[a][Re] = 1.0×10^{-4} M, $[NCS^-]$ = (2.0×10^{-2})−(2.0×10^{-1}) M, λ = 265 nm. [b]Spectrophotometrically determined from Abs vs $[NCS^-]$ data (eq 3), 25.0 °C, Figure 6b. [c]Obtained from global fit of the data reported in Figure 5b.

dx.doi.org/10.1021/ic301891u | *Inorg. Chem.* 2012, 51, 11996−12006

Table 5. Summary of the Kinetic Data for the Reaction between *fac*-[Re(Trop)(CO)$_3$(H$_2$O)]/*fac*-[Re(Trop)(CO)$_3$(MeOH)] and NCS$^-$ Ions at 25.0 °C in Water and Methanol, Respectively, at 25.0 °C[a]

	k_1 (M^{-1} s^{-1})	k_{-1} (s^{-1})	K_1 (M^{-1})	$\Delta H^{\ddagger}_{k1}$ (kJ mol^{-1})	$\Delta S^{\ddagger}_{k1}$ (J K^{-1} mol^{-1})
fac-[Re(Trop)(CO)$_3$(MeOH)]	0.268 ± 0.002	0.0044 ± 0.0002	61 ± 3 52 ± 4[b]	64 ± 1	−43 ± 5
fac-[Re(Trop)(CO)$_3$(H$_2$O)]	2.54 ± 0.03	0.0077 ± 0.0005	330 ± 22 207 ± 14[b]	56.1 ± 0.7	−49 ± 2

[a][Re] = 5 × 10^{-5} M, [NCS$^-$] = (2.5 × 10^{-3})−(3 × 10^{-2}) M, pH 6.4, λ = 260 nm, μ = 1 M (NaClO$_4$) for *fac*-[Re(Trop)(CO)$_3$(H$_2$O)] in water. [Re] = 1.0 × 10^{-4} M, [NCS$^-$] = (2.0 × 10^{-2})−(2.0 × 10^{-1}) M, λ = 265 nm, for *fac*-[Re(Trop)(CO)$_3$(MeOH)] in MeOH. [b]Spectrophotometrically determined from Abs vs [NCS$^-$] data (eq 3) (Figure 6).

Table 6. Summary of rate Constants for Methanol Substitution Reactions between *fac*-[Re(Trop)(CO)$_3$(MeOH)], *fac*-[Re(TropBr$_3$)(CO)$_3$(MeOH)], and *fac*-[Re(Flav)(CO)$_3$(MeOH)] with Various Monodentate Entering Ligands

	ligand	k_1 (M^{-1} s^{-1})	k_{-1} (s^{-1})	K_1 (M^{-1})	refs
fac-[Re(Trop)(CO)$_3$(H$_2$O)]	NCS$^-$	2.54 ± 0.03	0.0077 ± 0.0005	330 ± 22	this work
fac-[Re(Trop)(CO)$_3$(MeOH)]	NCS$^-$	0.268 ± 0.002	0.0044 ± 0.0002	61 ± 3	this work
fac-[Re(TropBr$_3$)(CO)$_3$(MeOH)]	Br$^-$	0.0706 ± 0.0004	0.004 ± 0.001	18 ± 4	19
	Py	0.0203 ± 0.0007	0.0016 ± 0.0002	12 ± 2	19
	DMAP	0.0345 ± 0.0007	0.00026 ± 0.00002	133 ± 11	19
fac-[Re(Flav)(CO)$_3$(MeOH)]	Br$^-$	7.2 ± 0.3	3.17 ± 0.09	2.5 ± 0.2	19
	Py	1.38 ± 0.08	0.0003 ± 0.0001	4600 ± 100	19
	DMAP	5.1 ± 0.2	0.00016 ± 0.00004	32000 ± 8000	19

using a prepared kit, following the [2 + 1] approach. In Table 5, the data for the aqua and methanol substitution reactions are summarized. It is clear that the rate of the aqua substitution reaction in water is almost 10 times faster than that of the coordinated methanol substitution in methanol, as illustrated by the k_1 values. Furthermore, the stability constant for the aqua substitution is ∼7 times larger than that of the methanol substitution reaction. These are excellent results, since it demonstrates that the aqua complex is more reactive and its product more stable than the corresponding methanol complex. Also, this might indicate that the aqua complexes of this type, *fac*-[Re(L,L′-Bid)(CO)$_3$(H$_2$O)] (L,L′-Bid = bidentate ligands), will possibly have better potential during radiolabeling processes, with faster reactions and more stable products.

Of additional interest is the fact that although the forward rate constants for aqua substitution from *fac*-[Re(Trop)-(CO)$_3$(H$_2$O)] by NCS$^-$ ions and the methanol substitution from *fac*-[Re(Trop)(CO)$_3$(MeOH)] by NCS$^-$ ions (k_1) differ by almost an order of magnitude (Table 6), the solvolysis rate constants (k_{-1}) of the corresponding thiocyanate ligand from *fac*-[Re(Trop)(CO)$_3$(NCS)] are very similar at 0.0077 ± 0.0005 vs 0.0044 ± 0.0002 s^{-1}, for aqua and methanol as entering ligands, respectively. This might indicate more toward dissociative activation. However, more data is required to more reliably confirm this observation.

Kinetic studies related to this reaction produced the following results: in the study by Smith et al.,[54] the substitution reactions between the metal complexes [Re(NO)(H$_2$O)-(CN)$_4$]$^{2-}$ and [Re(NO)(OH)(CN)$_4$]$^{3-}$ and the nucleophiles NCS$^-$, N$_3^-$, and thiourea (TU) were followed. In this case it was found that both the aqua and the hydroxo ligands are substituted.

The rate constants for the aqua substitution were determined as k_1(NCS$^-$) = (1.08 ± 0.03) × 10^{-3} M^{-1} s^{-1}, k_{-1}(NCS$^-$) = (6.3 ± 0.8) × 10^{-5} s^{-1}, k_1(N$_3^-$) = (1.9 ± 0.1) × 10^{-3} M^{-1} s^{-1}, k_{-1}(N$_3^-$) = (7 ± 4) × 10^{-5} s^{-1}, k_1(TU) = (1.05 ± 0.02) × 10^{-3} M^{-1} s^{-1}, and k_{-1}(TU) = (17 ± 5) × 10^{-5} s^{-1}. Purcell et al.[55] studied the aqua substitution reaction of [ReO(H$_2$O)(CN)$_4$]$^{1-}$ with NCS$^-$ as entering ligand. The rate constants obtained were k_1 = (3.48 ± 4) × 10^{-3} M^{-1} s^{-1} and k_{-1} = −3(2) × 10^{-5} s^{-1}. The oxygen exchange on this system was monitored by ^{17}O NMR.[56] The aqua complex was found to be far more reactive toward exchange [k_1(H$_2$O) = (9.1 ± 0.1) × 10^{-2} M^{-1} s^{-1}] compared to the hydroxo complex under the same conditions [k_1(OH) = (2.6 ± 0.3) × 10^{-3} M^{-1} s^{-1}]. No reaction was seen for the dioxo species. The cyanide exchange was later on monitored by means of ^{13}C and ^{15}N NMR.[57,58] For the dioxo species, [ReO$_2$(CN)$_4$]$^{3-}$, k_1 = (3.6 ± 0.3) × 10^{-6} M^{-1} s^{-1}, and for the aqua species, [ReO(H$_2$O)(CN)$_4$]$^-$, k_1 < 4 × 10^{-8} M^{-1} s^{-1}. However, the water substitution by a cyanide ligand was a much faster reaction with k_1 = 0.0035 M^{-1} s^{-1}.

The reactivity of the complexes studied in the current investigation, i.e., the aqua and methanol substitution, are significantly faster (2−3 orders of magnitude) than the water substitution in the [Re(NO)(H$_2$O)(CN)$_4$]$^{2-}$ and [ReO(H$_2$O)-(CN)$_4$]$^-$ complexes above. This indicates that the Re(I) carbonyl complexes reported here are much more labile toward substitution than the Re(III) and Re(V) complexes, in similar environments. This might be considered as some overarching evidence for more dissociative behavior.

As indicated above, a definite conclusion regarding the activation in the intimate mechanism, based on the values for $\Delta S^{\ddagger}$,[59] is not conclusive. The results from the coordinated methanol substitution by pyridine, 4-dimethylaminopyridine (DMAP), and bromide ions in methanol at 25.0 °C for two other complexes namely, *fac*-[Re(TropBr$_3$)(CO)$_3$(MeOH)] and *fac*-[Re(Flav)(CO)$_3$(MeOH)], is also included in Table 6.[19] It seems that there is an overall factor of 10 difference in rate obtained for the substitution reactions of *fac*-[Re-(TropBr$_3$)(CO)$_3$(MeOH)] compared to that of *fac*-[Re(Trop)-(CO)$_3$(MeOH)]. For the complex with 3-hydroxyflavone as bidentate ligand, *fac*-[Re(Flav)(CO)$_3$(MeOH)], the methanol substitution reactions is ∼2−5 times faster than that of *fac*-[Re(Trop)(CO)$_3$(MeOH)]. Since the entering ligands used are not consistent throughout, and taking into account that charged ligands vs neutral ligands might show different effects, it is clear

dx.doi.org/10.1021/ic301891u | Inorg. Chem. 2012, 51, 11996−12006

that overall the k_1 values of the methanol substitution reactions follow the following trend: *fac*-[Re(TropBr$_3$)(CO)$_3$(MeOH)] < *fac*-[Re(Trop)(CO)$_3$(MeOH)] < *fac*-[Re(Flav)-(CO)$_3$(MeOH)].

CONCLUSIONS

This study reports the first coordinated aqua substitution kinetic investigation on complexes of the type *fac*-[Re(L,L′-Bid)(CO)$_3$(H$_2$O)] in aqueous medium. The *O*,*O*′-bidentate ligand system used here allowed us to evaluate the reactivity of these types of complexes in water, which is of paramount importance for biomedical applications.

The substitution of H$_2$O by thiocyanate ions in water is faster than the respective reaction for methanol substitution in methanol (water vs methanol; 1 order of magnitude activation). This could possibly be indicative of an I$_d$ activation mechanism, where different leaving groups should have effects on the forward rate constant. In support of this, the reverse reaction rate constants, where NCS$^-$ is the leaving group in both cases, are fairly similar.

The influence of the tropolonato ligand and its induced reactivity fits perfectly to previously published work [the value of k_1 obtained for both media fall in the general trend observed before, i.e., k_1(*N*,*N*′-Bid) < k_1(*N*,*O*-Bid) < k_1(*O*,*O*′-Bid) (*N*,*N*′-Bid = 1,10-phenanthroline, 2,2′-bipyridine; *N*,*O*-Bid = (2-picolinate,2-quinolinate, 2,4-pyridinedicarboxylate, 2,4-quinolinedicarboxylate; *O*,*O*′-Bid = tribromotropolonate and 3-hydroxyflavonate]; however, this study needs to be expanded to a larger range of entering ligands and bidentate ligand systems and should include high-pressure mechanistic studies. More studies in water as solvent will also allow the evaluation of the Bronstedt pK_a of the coordinated aqua species and correlation with the different bidentate ligands used and their relative reactivities.

ASSOCIATED CONTENT

Supporting Information

Supplementary crystallographic data for **1** and **2** (CIF format) and tables of additional kinetic data. This material is available free of charge via the Internet at http://pubs.acs.org. CIF files CCDC 897501 and CCDC 897502 have also been submitted to The Cambridge Crystallographic Data Centre and can be obtained free of charge via the Internet at www.ccdc.cam.ac.uk/data_request/cif.

AUTHOR INFORMATION

Corresponding Author

*E-mail: visserhg@ufs.ac.za.

Notes

The authors declare no competing financial interest.

ACKNOWLEDGMENTS

We would like to thank Dr. Bernard Spingler from the University of Zurich and Mr. Theunis Muller from the University of the Free State for the crystal data collection and refinement. Financial assistance from the University of the Free State is gratefully acknowledged. We also express our gratitude toward SASOL, PETLabs Pharmaceuticals, the South African National Research Foundation (SA-NRF/THRIP), and the University of the Free State Strategic Academic Initiative (Advanced Biomolecular Systems) for financial support of this project. Opinions, findings, conclusions, or recommendations expressed in this material are those of the authors and do not necessarily reflect the views of the SA NRF.

REFERENCES

(1) Zobi, F.; Blacque, O.; Sigel, R. K. O.; Alberto, R. *Inorg. Chem.* **2007**, *46*, 10458−10460.
(2) Spingler, B.; Mundwiler, S.; Ruiz-Sanchez, P.; van Staveren, D. R.; Alberto, R. *Eur. J. Inorg. Chem.* **2007**, *18*, 2641−2647.
(3) Alberto, R.; Schibli, R.; Schubiger, P. A.; Abram, U.; Kaden, T. A. *Polyhedron* **1996**, *15*, 1079−1089.
(4) Abram, U.; Abram, S.; Alberto, R.; Schibli, R. *Inorg. Chim. Acta* **1996**, *248*, 193−202.
(5) Alberto, R.; Herrmann, W. A.; Kiprof, P.; Baumgartner, F. *Inorg. Chem.* **1992**, *31*, 895−899.
(6) Alberto, R.; Schibli, R.; Waibel, R.; Abram, U.; Schubiger, A. P. *Coord. Chem. Rev.* **1999**, *190−192*, 901−919.
(7) Raposinho, P. D.; Correia, J. D. G.; Alves, S.; Botelho, M. F.; Santos, A. C.; Santos, I. *Nucl. Med. Biol.* **2008**, *35*, 91−99.
(8) Isolink kit, Mallinckrodt-Covidien, Petten, The Netherlands.
(9) Alberto, R.; Ortner, K.; Wheatley, N.; Schibli, R.; Schubiger, A. P. *J. Am. Chem. Soc.* **2001**, *123*, 3135−3136.
(10) Schibli, R.; Schwarzbach, R.; Alberto, R.; Ortner, K.; Schmalle, H.; Dumas, C. *Bioconjugate Chem.* **2002**, *13*, 750−756.
(11) Mundwiler, S.; Kundig, M.; Ortner, K.; Alberto, R. *J. Chem. Soc., Dalton Trans.* **2004**, *9*, 1320−1328.
(12) Gorshkov, N. I.; Schibli, R.; Schubiger, A. P.; Lumpov, A. A.; Miroslavov, A. E.; Suglobov, D.N. J. *Organomet. Chem.* **2004**, *689*, 4757−4763.
(13) Riondato, M.; Camporese, D.; Martin, D.; Suades, J.; Alvarez-Lorena, A.; Mazzi, U. *Eur. J. Inorg. Chem.* **2005**, 4048−4055.
(14) Agorastos, N; Borsig, L.; Renard, A.; Antoni, P.; Viola, G.; Spingler, B.; Kruz, P.; Alberto, R. *Chem.—Eur. J.* **2007**, *13*, 3842−3852.
(15) Gorshkov, N. I.; Lumpov, A. A.; Miroslavov, A. E.; Suglobov, D. N. *Radiochemistry* **2005**, *47*, 45−49.
(16) Salignac, B.; Grundler, P. V.; Cayemittes, S.; Frey, U.; Scopelliti, R.; Merbach, A. *Inorg. Chem.* **2003**, *42*, 3516−3526.
(17) Grundler, P. V.; Salignac, B.; Cayemittes, S.; Alberto, R.; Merbach, A. E. *Inorg. Chem.* **2004**, *43*, 865−873.
(18) Grundler, P. V.; Helm, L.; Alberto, R.; Merbach, A. E. *Inorg. Chem.*. **2006**, *45*, 10378−10390.
(19) Schutte, M.; Kemp, G.; Visser, H. G.; Roodt, A. *Inorg. Chem.* **2011**, *50* (24), 12486−12498.
(20) Alberto, R. *Top. Curr. Chem.* **2005**, *252*, 1−44.
(21) *MicroMath Scientist for Windows, Version 2.01*,MicroMath, Inc., 1986−1995.
(22) *Microsoft Office 2007*; Microsoft Corp., 2011.
(23) *CrysAlis^{Pro} Software System, Version 171.32*; Oxford Diffraction Ltd.: Oxford, UK, 2007.
(24) *SAINT-Plus, version 6.02 (including XPREP)*; Bruker AXA, Inc.: Madison, WI, 1999.
(25) *SADABS, version 2004/1*; Bruker AXS, Inc.: Madison, WI, 2004.
(26) Altomare, A.; Burla, M. C.; Camalli, M.; Cascarano, G. L.; Giacovazzo, C.; Guagliardi, A.; Moliterni, A. G. G.; Polidori, G.; Spagna, R. *J. Appl. Crystallogr.* **1999**, *32*, 115−119.
(27) Sheldrick, G. M. *Acta Crystallogr.* **2008**, *A64*, 112−122.
(28) Farrugia, L. J. *J. Appl. Crystallogr.* **1999**, *32*, 837−838.
(29) Spek, A. L. *J. Appl. Crystallogr.* **2003**, *36*, 7−13.
(30) Brandenburg, K., Putz, H. *DIAMOND, release 3.1b*, Crystal Impact GbR: Bonn, Germany, 2005.
(31) Herbst-Irmer, R.; Sheldrick, G. M. *Acta Crystallogr.* **1998**, *B54*, 443−449.
(32) Brink, A.; Visser, H. G.; Roodt, A. *J. Coord. Chem.* **2011**, *64*, 122−133.
(33) Herbst-Irmer, R.; Sheldrick, G. M. *Acta Crystallogr.* **1998**, *B54*, 443−449.
(34) Schutte, M.; Visser, H. G.; Roodt, A. *Acta Crystallogr.* **2010**, *E66*, m859−m860.

(35) Brasey, T.; Buryak, A.; Scopelliti, R.; Severin, K. *Eur. J. Inorg. Chem.* **2004**, 964−967.
(36) Schutte, M.; Visser, H. G.; Roodt, A. *Acta Crystallogr.* **2007**, *E63*, m3195−m3196.
(37) Schutte, M.; Visser, H. G.; Roodt, A. *Acta Crystallogr.* **2008**, *E64*, m1610−m1611.
(38) Benny, P. D.; Fugate, G. A.; Barden, A. O.; Morley, J. E.; Silva-Lopez, E.; Twamley, B. *Inorg. Chem.* **2008**, *47*, 2240−2242.
(39) Casanova, M.; Zangrondo, E.; Munini, F.; Iengo, E.; Alessio, E. *Dalton Trans.* **2006**, 5033−5045.
(40) Franklin, B. R.; Herrick, R. S.; Ziegler, C. J.; Cetin, A.; Barone, N.; London, L. R. *Inorg. Chem.* **2008**, *47*, 5902−5909.
(41) Herrick, R. S.; Ziegler, C. J.; Cetin, A.; Franklin, B. R. *Eur. J. Inorg. Chem.* **2007**, 1632−1634.
(42) Cambridge Structural Database (CSD), Version 5.32, Feb 2011 update. Allen, F. H. *Acta Crystallogr.* **2002**, *B58*, 380.
(43) Purcell, W.; Roodt, A.; Basson, S. S.; Leipoldt, J. G. *Transition Met. Chem.* **1990**, *15*, 239−241.
(44) Purcell, W.; Roodt, A.; Basson, S. S.; Leipoldt, J. G. *Transition Met. Chem.* **1989**, *14*, 5−6.
(45) Roodt, A.; Visser, H. G.; Brink, A. *Crystallogr. Rev.* **2011**, *17*, 241−280.
(46) Roodt, A.; Abou-Hamdan, A.; Engelbrecht, H. P.; Merbach, A. E. *Adv. Inorg. Chem.* **1999**, *40*, 59−126.
(47) Cotton, F. A., Wilkinson, G., Gaus, P. L. *Basic Inorganic Chemistry*, 3rd ed.; John Wiley & Sons Inc.: London, U.K., 1995.
(48) Crous, R.; Datt, M.; Foster, D.; Bennie, L.; Steenkamp, C.; Huyser, J.; Kirsten, L.; Steyl, G.; Roodt, A. *Dalton Trans.* **2005**, 1108−1116.
(49) Otto, S.; Roodt, A. *Inorg. Chim. Acta* **2004**, *357*, 1−10.
(50) Roodt, A.; Otto, S.; Steyl, G. *Coord. Chem. Rev.* **2003**, *245*, 125−142.
(51) Brink, A.; Visser, H. G.; Roodt, A.; Steyl, G. *Dalton Trans.* **2010**, *39*, 5572−5578.
(52) Egli, A.; Hegetschweiler, K.; Alberto, R.; Abram, U.; Schibli, R.; Hedinger, R.; Gramlich, V.; Kissner, R.; Schubiger, P. A. *Organometallics* **1997**, *16*, 1833−1840.
(53) Evans, M. G.; Polanyi, M. *Trans. Faraday Soc.* **1935**, *31*, 875−894.
(54) Smith, J.; Purcell, W.; Lamprecht, G. J.; Roodt, A. *Polyhedron* **1996**, *15*, 1389−1395.
(55) Purcell, W.; Roodt, A.; Basson, S. S.; Leipoldt, J. G. *Transition Met. Chem.* **1989**, *14*, 224−226.
(56) Roodt, A.; Leipoldt, J. G.; Helm, L.; Abou-Hamdan, A.; Merbach, A. E. *Inorg. Chem.* **1995**, *34*, 560−568.
(57) Roodt, A.; Abou-Hamdan, A.; Engelbrecht, H. P.; Merbach, A. E. *Inorg Chem.* **1999**, *40*, 59−126.
(58) Abou-Hamdan, A.; Roodt, A.; Merbach, A. E. *Inorg. Chem.* **1998**, *37*, 1278−1288.
(59) Schutte, M. Ph.D. Thesis, University of the Free State, 2011.